Supplemental Information & Figures

Comprehensive Lipidome Profiling of Isogenic Primary and Metastatic Colon
Adenocarcinoma Cell Lines

Cassie J. Fhaner[1], Sichang Liu[1], Hong Ji[2], Richard J. Simpson[2] and Gavin E. Reid[1,3*]

[1]Department of Chemistry, Michigan State University, 578 S. Shaw Lane, East Lansing, Michigan, USA, 48824; [2]Department of Biochemistry, La Trobe University, Victoria, Australia, 3086; [3]Department of Biochemistry and Molecular Biology, Michigan State University, 603 Wilson Road, East Lansing, Michigan, USA, 48824

* Corresponding Author: Chemistry Building, 578 S. Shaw Lane. Room 229, Michigan State University, East Lansing, Michigan, USA, 48824. Phone: 517-355-9715 x198; Email: reid@chemistry.msu.edu

Supplemental Materials and Methods

Reagents: RPMI 1640 medium, penicillin and streptomycin antibiotic mix and 0.25% Trypsin-EDTA were obtained from Invitrogen (Carlsbad, CA). LC grade water, methanol (MeOH), chloroform ($CHCl_3$) and ACS grade isopropanol (IPA) were purchased from Macron Chemicals (Center Valley, PA). N,N-dimethylformamide (DMF) and triethylamine (TEA) were from Jade Scientific (Westland, MI). Ammonium formate was obtained from Alfa Aesar (Ward Hill, MA). 99% formic acid was purchased from Spectrum Scientific (Irvine, CA). Synthetic lipid standards were from Avanti Polar Lipids, Inc. (Alabaster, AL).

Cell Culture: SW480 and SW620 cells were routinely cultured in RPMI1640 medium supplemented with 10% FCS, 100 unit/mL penicillin and 100µg/mL streptomycin at 37°C and 10% CO_2 atmosphere. Approximately 2×10^6 cells of each cell line were seeded into 150mm diameter culture dish containing 25mL of the culture medium and cultured until cell density reached 70-80% confluence. Cells were washed three times with ice-cold PBS and lifted off the culture plates with 0.25% Trypsin-EDTA. Cell suspensions were then centrifuged at 400g and the cell pellets were washed once with ice-cold PBS. Approximately 2×10^7 cells of each cell line were resuspended in 1 mL of PBS, snap frozen and lyophilized.

Mass Spectrometry Analysis: Samples were loaded into a Whatman multichem 96-well plate (Sigma Aldrich, St. Louis, MO) and sealed with Teflon Ultra Thin Sealing Tape (Analytical Sales and Services, Prompton Plains, NJ). The spray voltage used on the Advion Triversa Nanomate was 1.4 kV, with a gas pressure of 0.3 psi. The ion source interface settings (inlet temperature of 100^oC and S-Lens value of 50%) were optimized to maximize the sensitivity of the precursor ions while minimizing 'in-source' fragmentation. High resolution mass spectra were acquired across the range of m/z from 200-2000, and were signal averaged for 3 minutes. Mass spectra were initially acquired at a range of different dilutions of the lipid extracts to determine the range at which linearity in the response of specific lipids was observed, and to ensure that the ratio of specific lipid ion abundances compared to other lipids within the mixture, or compared to the internal standards, remained constant. External calibration of the instrument was initially performed using the standard Thermo LTQ calibration mixture. To characterize the individual acyl, plasmanyl and/or plasmenyl alkyl chain compositions and degree of unsaturation within specific identified lipid ions from the underivatized sample, Higher-Energy Collision

Induced Dissociation (HCD-MS/MS) product ion spectra were acquired in positive and/or negative ionization mode on monoisotopically isolated precursor ions using the FT analyzer (100,000 resolving power), with default activation times and a low mass limit of m/z 100. In selected cases, to confirm the presence and identity of plasmenyl- or plasmanyl-ether containing lipids, ion trap CID-MS/MS and -MS^n experiments were performed using an activation time of 10 ms and an activation q value of 0.25. Automated Gain Control (AGC) target numbers were maintained at the default settings for all MS and MS/MS experiments. In all cases, normalized collision energies were optimized for each precursor ion to maximize the intensity of the most abundant product ion within the observable m/z range. MS/MS spectra were signal averaged for 30-60 seconds, depending on the precursor ion abundance.

For the phospholipids, HCD-MS/MS was performed in negative ionization mode on the deprotonated precursor ions, with the exception of PC lipids, which were analyzed as their formate adducts. Similarly, the sphingolipids were also analyzed as their formate adducts in negative ionization mode[1]. It is important to note that formate adducts were employed here as opposed to the common acetate adduct, in order to eliminate the possibility of nominal mass overlap between the acetate adducts of ether-linked PC lipids with deprotonated ether-linked PE lipids. This is especially significant because the structural identification of ether-linked phospholipids relies heavily on observation of the acyl chain neutral loss product ions (see Supplemental Figure S14 for an example), and the fragments of ether PC and ether PE lipids containing 2 more carbons would have identical exact masses. For example, [PC$_{(O-16:1/16:0)}$+Ac]$^-$ and [PE$_{(O-18:0/22:6)}$-H]$^-$ both have a nominal m/z of 776. During negative ion fragmentation, the PC lipid initially loses methyl acetate, forming [dimethyl PE$_{(O-16:1/16:0)}$-H]$^-$, that subsequently dissociates via the loss of 16:0 R'CHCO and RCOOH fatty acyl chains to give rise to product ions at m/z 464.3141 and 446.3035, respectively, which would have the same exact m/z values as a PE ion that had lost 22:6 R'CHCO and RCOOH fatty acyl chains. However, as the m/z of the formate adduct is 14 Da less than the acetate adduct, this overlap is not problematic and MS/MS and MS^3 can be performed without ambiguity.

For the characterization of TG lipid ions, positive ion mode HCD-MS/MS (or CID-MS/MS followed by HCD-MS^3) spectra were acquired to observe the neutral loss of characteristic fatty acids from the ammonium ion adducts at each of the identified precursor ion m/z values for these lipids, as previously described[2]. The assignment of the fatty acyl chains for these lipids in Supplemental Table S12 are listed in order from the shortest to the longest acyl chain, and not in terms of their S$_N$ position. Unfortunately, the ammonium adducts for the ether

TG lipids and DG lipids were not sufficiently stable to allow their isolation for MS/MS or MS^3 analysis. Therefore, these species are expressed simply in terms of their sum compositions (i.e., the total number of carbons and double bonds).

Data Analysis: Post-acquisition offline calibration was performed using the Recalibration Offline software in Xcalibur (Thermo Scientific, San Jose, CA), using the calculated theoretical masses of the protonated PE$_{(14:0/14:0)}$, PC$_{(14:0/14:0)}$ and PS$_{(14:0/14:0)}$ internal standards, and an abundant PC$_{(36:2)}$ lipid present in the extract in positive ionization mode, and the calculated m/z values of the formate adducts of the internal standard PC$_{(28:0)}$ lipid, and the formate adduct of the PC$_{(34:2)}$ and deprotonated PA$_{(34:0)}$ and PI$_{(36:1)}$ lipids present in the extract in negative ionization mode (the identities of these lipids were all first confirmed using MS/MS). Peak lists containing the recalibrated masses and intensities were then transferred to Microsoft Excel, then lipid identification (i.e., assignment of the lipid headgroup, the nature of the linkage of the hydrophobic tails and the total number of carbons and degree of unsaturation) was performed using the Lipid Mass Spectrum Analysis (LIMSA) v.1.0 software linear fit isotope correction algorithm (available for free download from the University of Helsinki at http://www.helsinki.fi/science/lipids/software.html), in conjunction with an 'in-house' developed database of hypothetical lipid compounds inserted into the database as a list of ionic elemental compositions, for automated peak finding (using a peak width tolerance of 0.003 and a sensitivity of 0.01%) and for the correction of ^{13}C isotope effects. The database was restricted to protonated or ammoniated lipid ions, as the use of ammonium formate in the solvent, along with the lipid extraction procedure, was found to limit sodium adduct formation to a negligible amount. Peaks originally picked by LIMSA that were outside the 95% confidence level of the experimental mass accuracy (determined to be 2.57 ppm) were removed. Relative quantification of lipid ion abundances was performed by comparison of each lipid ion abundance compared to the ion abundance of the PC$_{(14:0/14:0)}$ internal standard. No attempts were made to quantitatively correct for different ESI responses of individual lipids due to concentration, acyl chain length or degree of unsaturation. Thus, the abundance of the ions corresponding to individual molecular species within each lipid class, normalized to the abundance of the PC$_{(14:0/14:0)}$ internal standard, are reported here as the percentage of the total lipid ion abundance for each class, and do not represent the absolute concentrations of each lipid or lipid class. The internal standards PE$_{(14:0/14:0)}$ and PS$_{(14:0/14:0)}$ were includedto monitor the completeness of the D$_6$-DMBNHS reaction. All lipid classes (PC, PE, PS, PG, PI, lysophosphatidylcholine (LPC),

lysophosphatidylethanolamine (LPE), lysophosphatidylserine (LPS), triradylglycerol (TG), diradylglycerol (DG), monoradylglycerol (MG), sphingomyelin (SM), ceramide (Cer), cholesterol (Chol) and cholesterol esters (Chol esters)) except for PA were identified and quantified from the d_6-DMBNHS derivatized spectra. Determination of the abundance of PA lipids was performed in negative ionization mode, then a correction was applied to the positive ion mode spectra to remove the contribution of these lipids to the PC lipid ion abundances (an appropriate correction factor was determined using the negative and positive ion abundances measured using a series of PA lipid standards analyzed under the same conditions as the lipid extracts). In the results described below, lipids whose identities of their headgroup and fatty acyl, alkyl and/or alkenyl chains could be unambiguously assigned by manual analysis of their individual MS/MS spectra are classified as 'Identified Lipids', while 'Total lipids' includes the combined number of 'Identified Lipids' as well as those lipids where only the total number of carbons and double bonds within the acyl, alkyl and/or alkenyl chains could be assigned from the high resolution d_6-DMBNHS derivatized and mild formic acid hydrolyzed ESI-MS data. Student's t-test with 2 tailed distribution, two sample unequal variance was used to evaluate differences in the individual ion abundances between the SW480 and SW620 cell line crude lipid extracts, with $p < 0.01$ considered statistically significant. Data are presented as mean ± standard deviation.

Nomenclature: Throughout this paper, the nomenclature used for lipid classification and structural representation is that recommended by the LIPID MAPS consortium[3,4]. For glycerophospholipids, the headgroup of the lipid subclass is followed by either (i) the combined total number of carbons and double bonds within the S_N1 and S_N2 chains (e.g. $PC_{(34:1)}$), or (ii) the total number of carbons and double bonds within the individual S_N1 and S_N2 chains, respectively (e.g., $PC_{(16:0/18:1)}$). The presence of plasmanyl-glycerophospholipids are noted with an 'O-' (e.g., 1-O-hexadecanyl-2-oleoyl-*sn*-glycero-3-phosphocholine is designated as $PC_{(O-16:0/18:1)}$), while plasmenyl-glycerophospholipids are noted with a 'P-' (e.g., 1-O-hexadecan-1'enyl-2-oleoyl-*sn*-glycero-3-phosphocholine is designated as $PC_{(P-16:0/18:1)}$). Lysoglycerophospholipids are designated with an upper case 'L' (e.g., LPC). For sphingolipids, Cer and SM lipids are noted with the sphingosine or sphinganine chain first denoted with a 'd' and the amide-linked acyl chain second (i.e. $SM_{(d18:1/16:0)}$) or as the total number of carbons and double bonds (i.e. $SM_{(34:1)}$). TG lipids are represented with the acyl chains placed in short to long chain order without regard to S_N linkage position or by total number of carbons and double bonds in the fatty acyl chains

with 'O-' for plasmanyl and 'P-' for plasmenyl where necessary. DG, MG and Chol esters are designated by the lipid subclass followed by the combined total number of carbons and double bonds within the fatty acyl chain(s).

Supplemental References:

1. Valsecchi, M.M.,L., Casellato, R., Prioni, S., Loberto, N., Prinetti, A., Chigorno, V. and Sonnino, S. *J. Lipid Res.,* **2007**. *48*, 417-424.
2. Busik, J.V., Reid, G.E. and Lydic, T.A. *Meth. Mol. Biol*. **2009**, *579,* 33-70.
3. Fahy, E., Subramaniam, S., Brown, H. A., Glass, C. K., Merrill Jr., A. H., Murphy, R. C., Raetz, C. R. H., Russell, D. W., Seyama, Y., Shaw, W., Shimizu, T., Spener, F., van Meer, G., VanNieuwenhze, M. S., White, S. H., Witztum, J. L., Dennis, E. A. J. Lipid Res. **2005**. 46, 839-861.
4. Fahy, E., Subramaniam, S., Murphy, R., Nishijima, M., Raetz, C., Shimizu, T., Spener, F., van Meer, G., Wakelam, M., Dennis, E. A. J. Lipid Res. **2009**. 50, S9-S14.
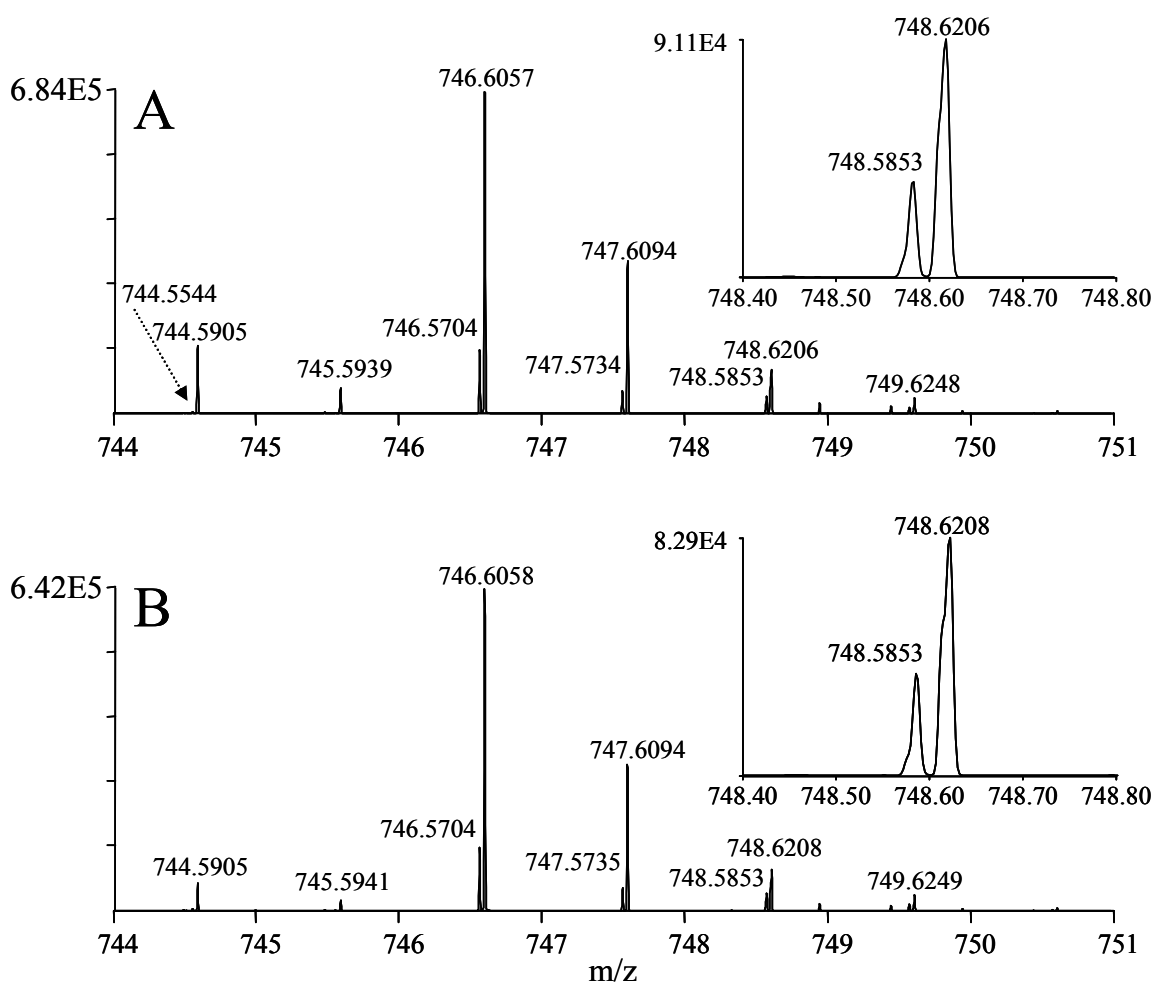
Figure S1. Positive ion mode ESI high-resolution mass spectrometric analysis of a crude lipid extract from the SW480 human adenocarcinoma cell line. (A) Expanded region (m/z 744-751) of the ESI-mass spectrum obtained after reaction with the amine-specific derivatization reagent, d_6-DMBNHS (from Figure 2A), and (B) Expanded region (m/z 744-751) of the ESI-mass spectrum obtained after reaction with d_6-DMBNHS followed by mild formic acid hydrolysis (from Figure 2B).
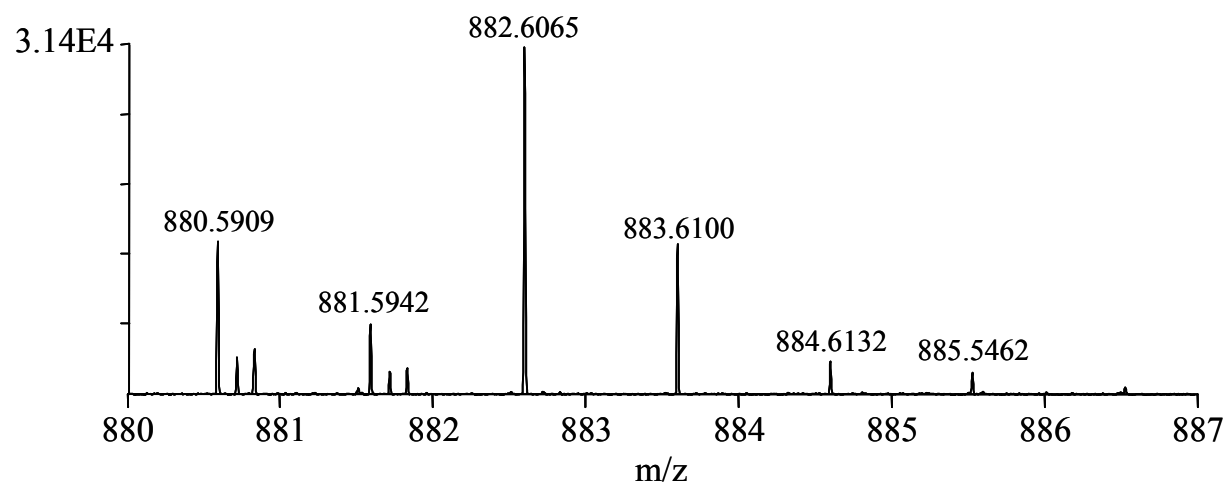
Figure S2. Positive ion mode ESI high-resolution mass spectrometric analysis of a crude lipid extract from the SW480 human adenocarcinoma cell line. Expanded region (m/z 880-887) of the ESI-mass spectrum from Figure 1A.
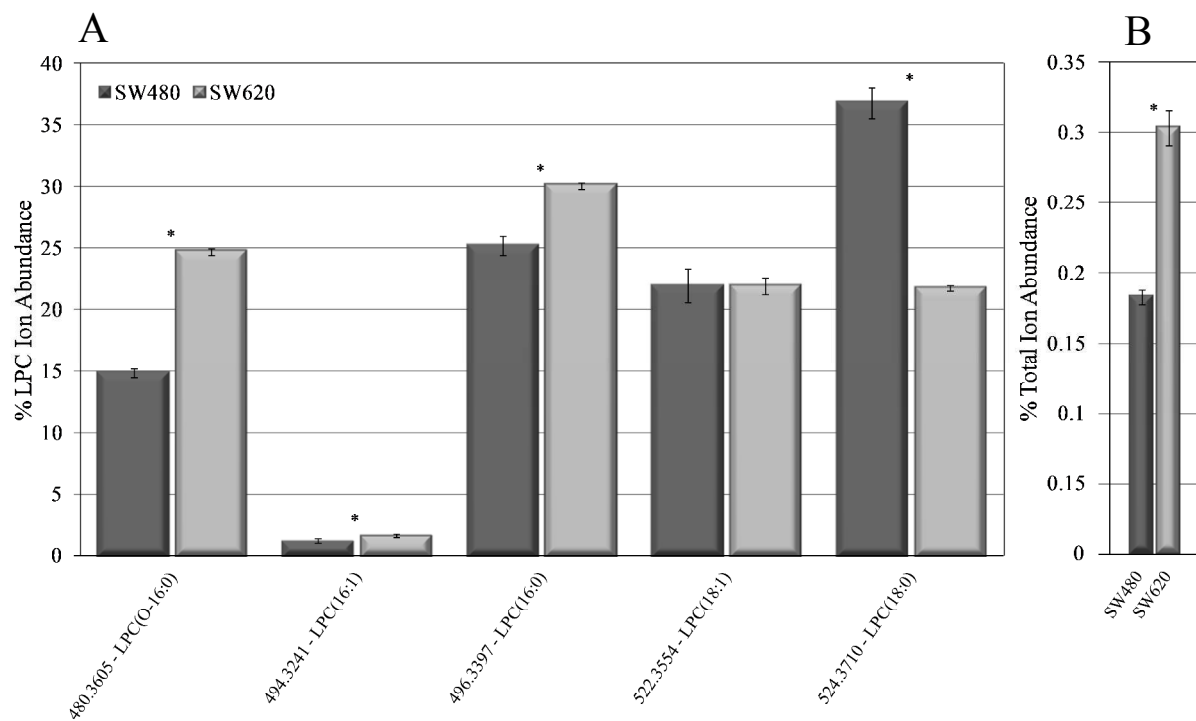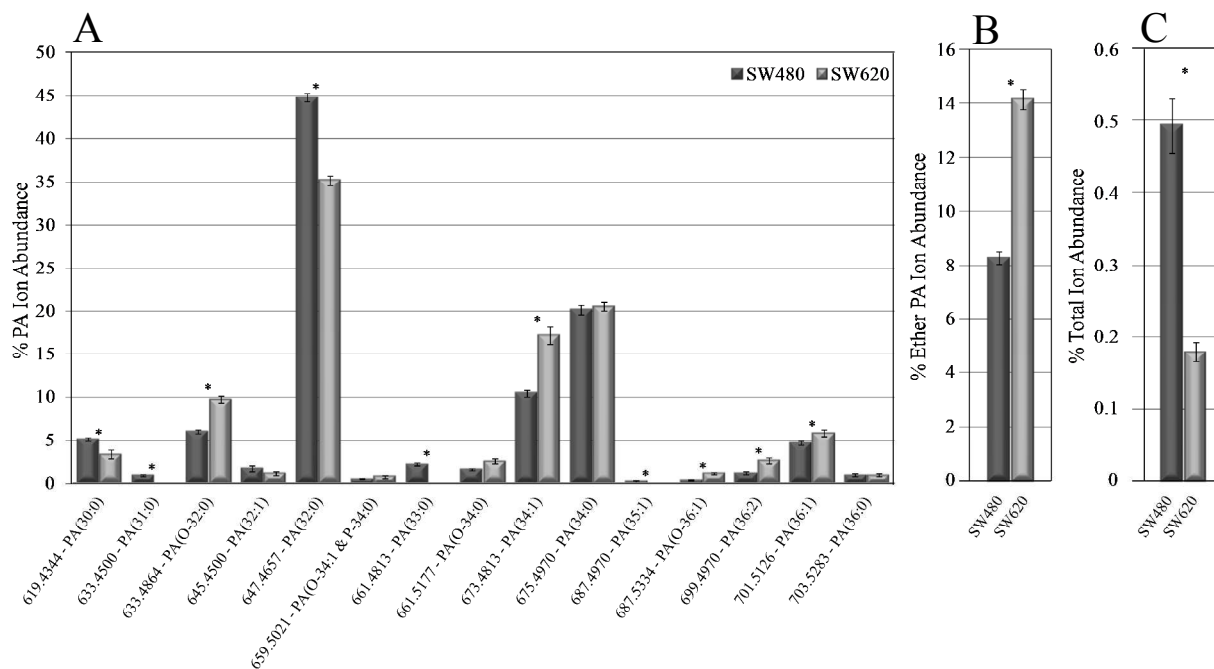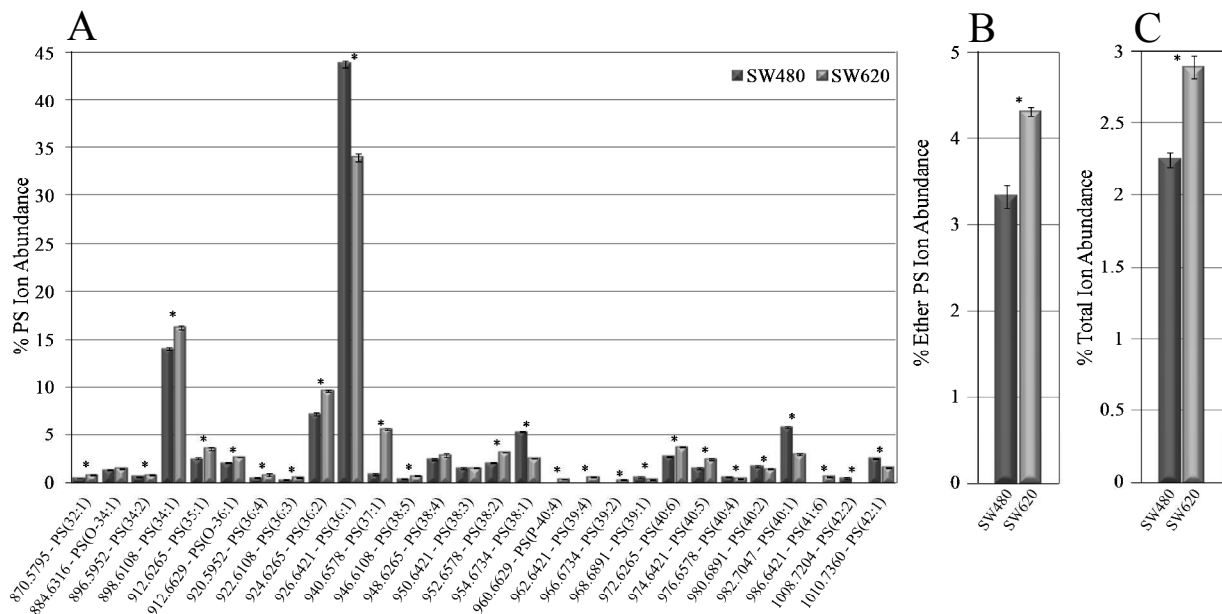
Figure S3. Quantification of LPC lipids from the d_6-DMBNHS derivatized SW480 and SW620 cell crude lipid extracts. (A) Percent individual LPC ion abundances compared to the total ion abundance for all LPC lipids. (B) Percent total LPC ion abundance compared to the total ion abundance for all identified lipids. n = 5, * = p < 0.01.
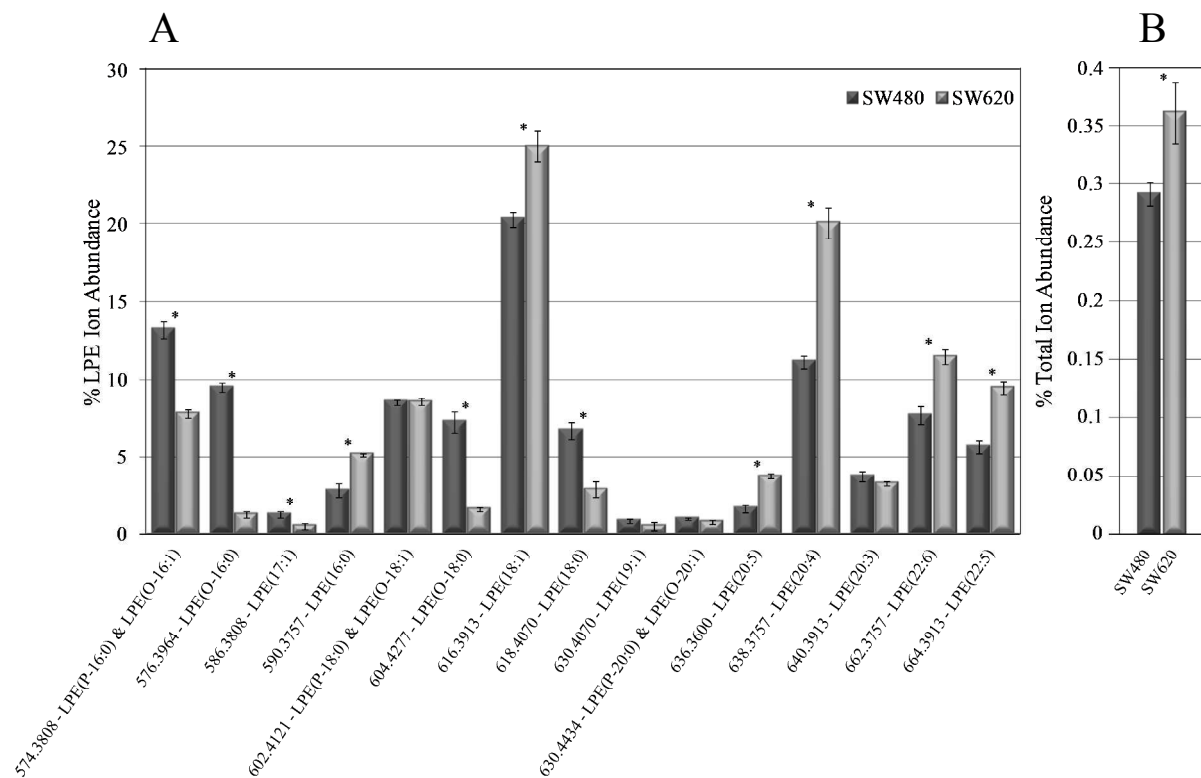
Figure S4. Quantification of LPE lipids from the d_6-DMBNHS derivatized SW480 and SW620 cell crude lipid extracts. (A) Percent individual LPE ion abundances compared to the total ion abundance for all LPE lipids. (B) Percent total LPE ion abundance compared to the total ion abundance for all identified lipids. n = 5, * = p < 0.01.

Figure S5. Quantification of PA lipids from the d_6-DMBNHS derivatized SW480 and SW620 cell crude lipid extracts. (A) Percent individual PA ion abundances compared to the total ion abundance for all PA lipids. (B) Percent total ether-linked PA ion abundance compared to the total PA lipid ion abundance. (C) Percent total PA ion abundance compared to the total ion abundance for all identified lipids. $n = 5$, * = $p < 0.01$.
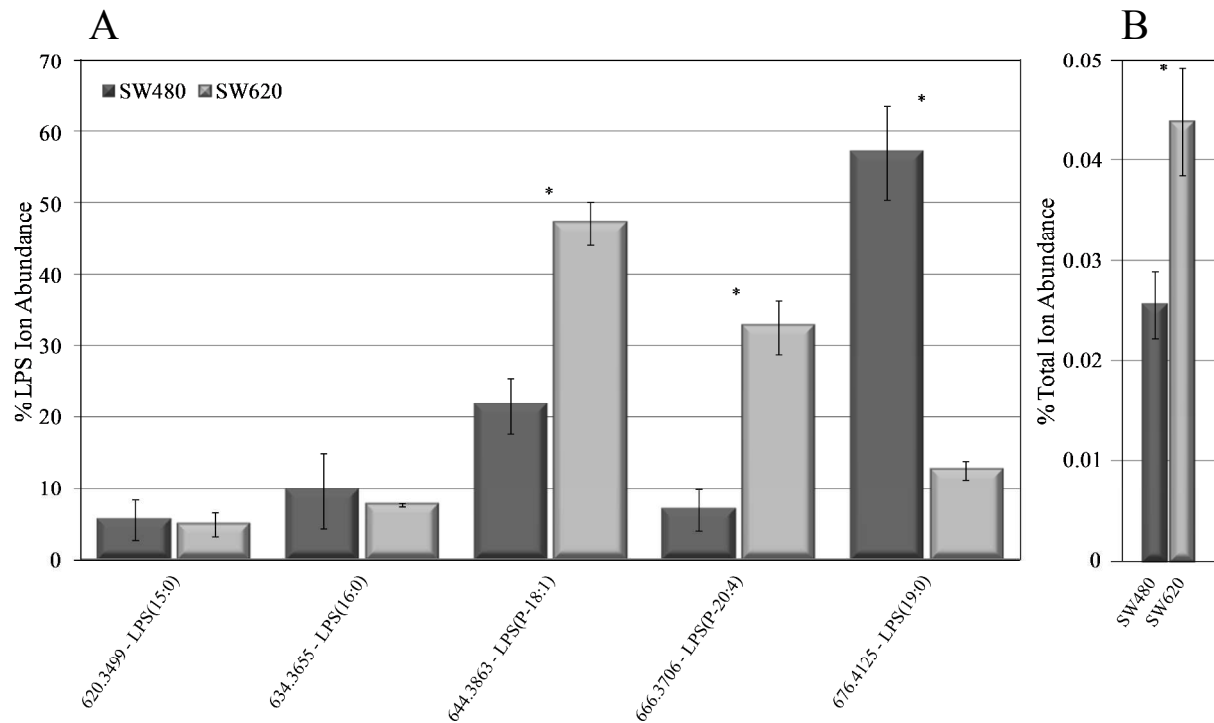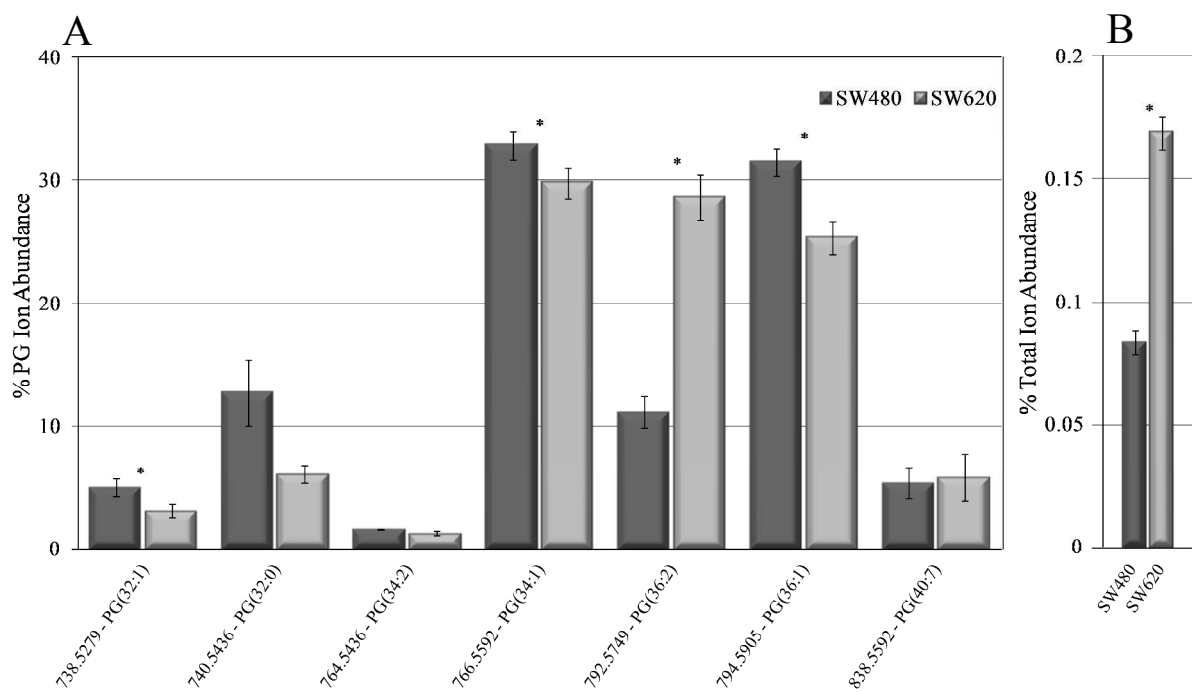
Figure S6. Quantification of PS lipids from the d_6-DMBNHS derivatized SW480 and SW620 cell crude lipid extracts. (A) Percent individual PS ion abundances compared to the total ion abundance for all PS lipids. (B) Percent total ether-linked PS ion abundance compared to the total PS lipid ion abundance. (C) Percent total PS ion abundance compared to the total ion abundance for all identified lipids. n = 5, * = p < 0.01.

Figure S7. Quantification of LPS lipids from the d_6-DMBNHS derivatized SW480 and SW620 cell crude lipid extracts. (A) Percent individual LPS ion abundances compared to the total ion abundance for all LPS lipids. (B) Percent total LPS ion abundance compared to the total ion abundance for all identified lipids. n = 5, * = p < 0.01.
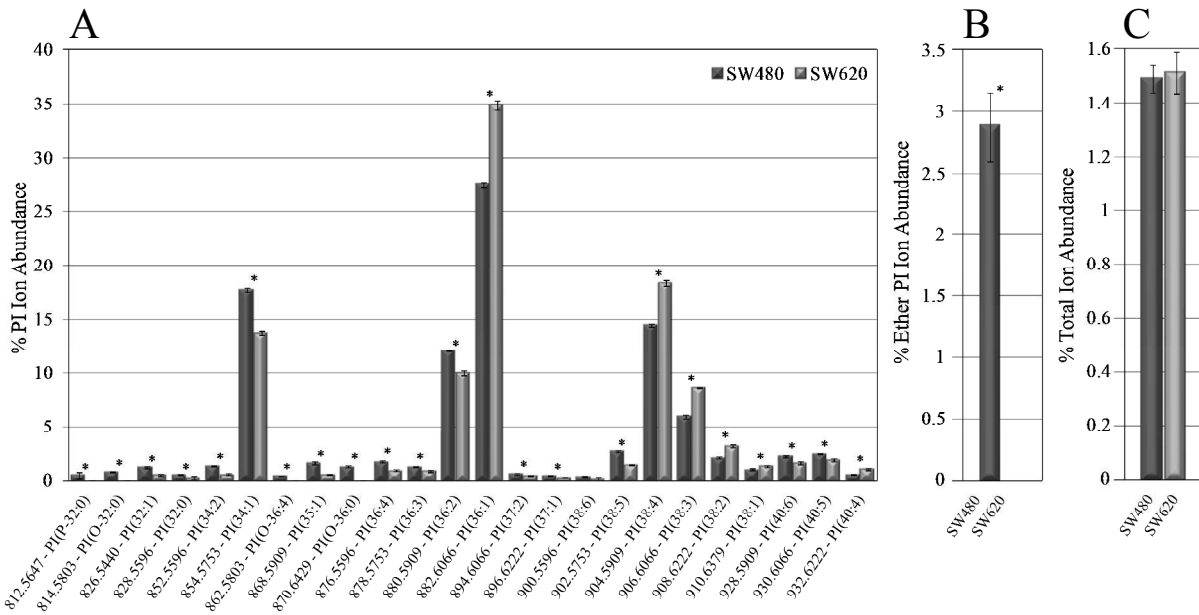
Figure S8. Quantification of PG lipids from the d_6-DMBNHS derivatized SW480 and SW620 cell crude lipid extracts. (A) Percent individual PG ion abundances compared to the total ion abundance for all PG lipids. (B) Percent total PG ion abundance compared to the total ion abundance for all identified lipids. n = 5, * = p < 0.01.

Figure S9. Quantification of PI phospholipids from the d_6-DMBNHS derivatized SW480 and SW620 cell crude lipid extracts. (A) Percent individual PI ion abundances compared to the total ion abundance for all PI lipids. (B) Percent total ether-linked PI ion abundance compared to the total PI lipid ion abundance. (C) Percent total PI ion abundance compared to the total ion abundance for all identified lipids. n = 5, * = p < 0.01.
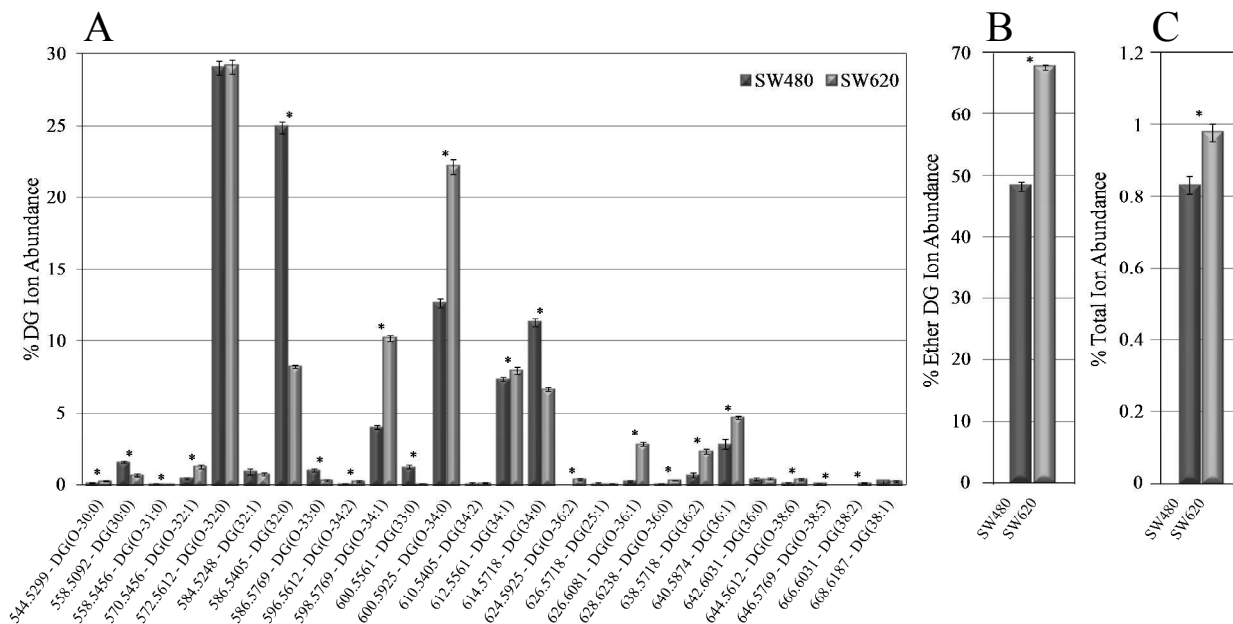
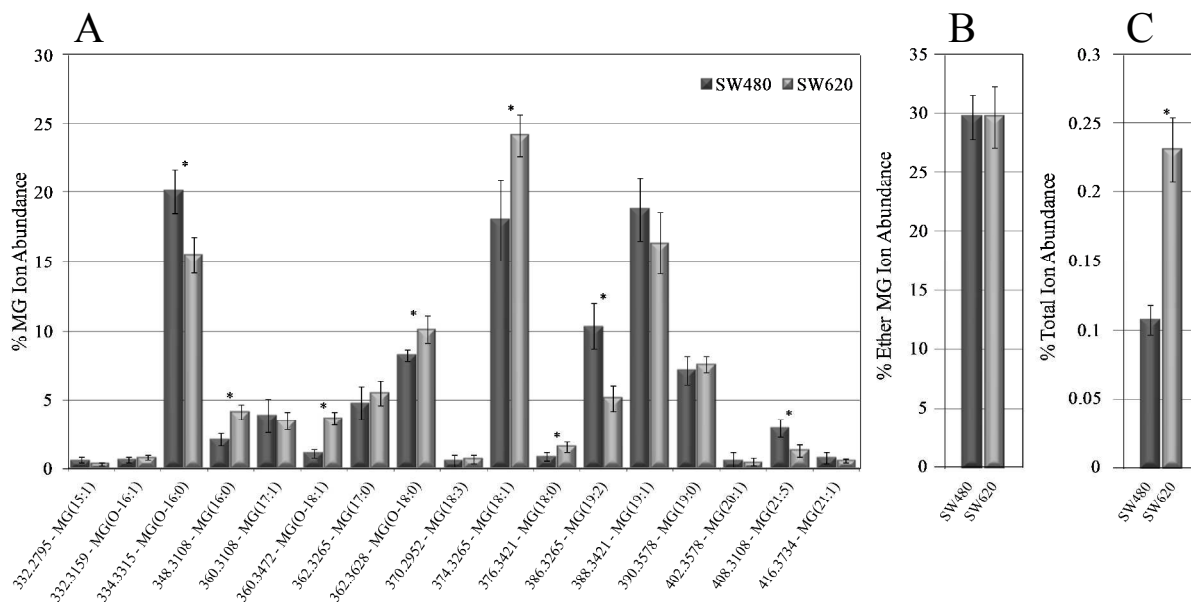**Figure S10.** Quantification of DG phospholipids from the d_6-DMBNHS derivatized SW480 and SW620 cell crude lipid extracts. (A) Percent individual DG ion abundances compared to the total ion abundance for all DG lipids. (B) Percent total ether-linked DG ion abundance compared to the total DG lipid ion abundance. (C) Percent total DG ion abundance compared to the total ion abundance for all identified lipids. n = 5, * = p < 0.01.
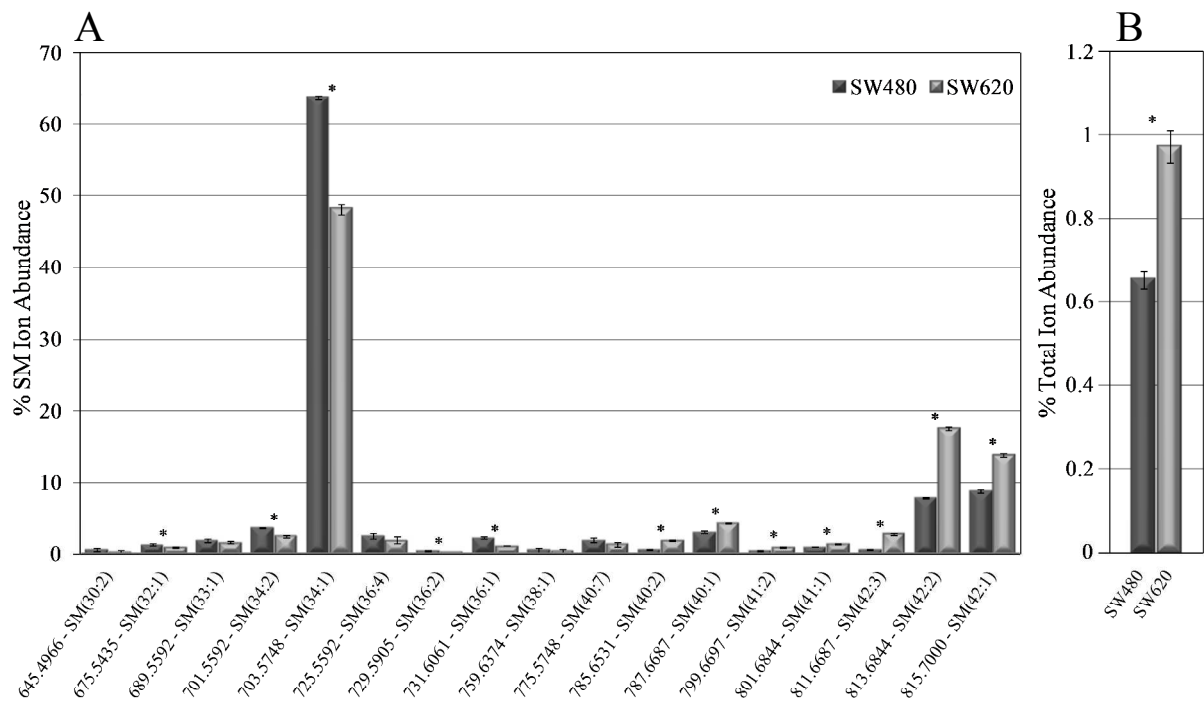
Figure S11. Quantification of MG phospholipids from the d_6-DMBNHS derivatized SW480 and SW620 cell crude lipid extracts. (A) Percent individual MG ion abundances compared to the total ion abundance for all MG lipids. (B) Percent total ether-linked MG ion abundance compared to the total MG lipid ion abundance. (C) Percent total MG ion abundance compared to the total ion abundance for all identified lipids. n = 5, * = p < 0.01.

Figure S12. Quantification of SM sphingolipids from the d_6-DMBNHS derivatized SW480 and SW620 cell crude lipid extracts. (A) Percent individual SM ion abundances compared to the total ion abundance for all SM lipids. (B) Percent total SM ion abundance compared to the total ion abundance for all identified lipids. n = 5, * = p < 0.01.
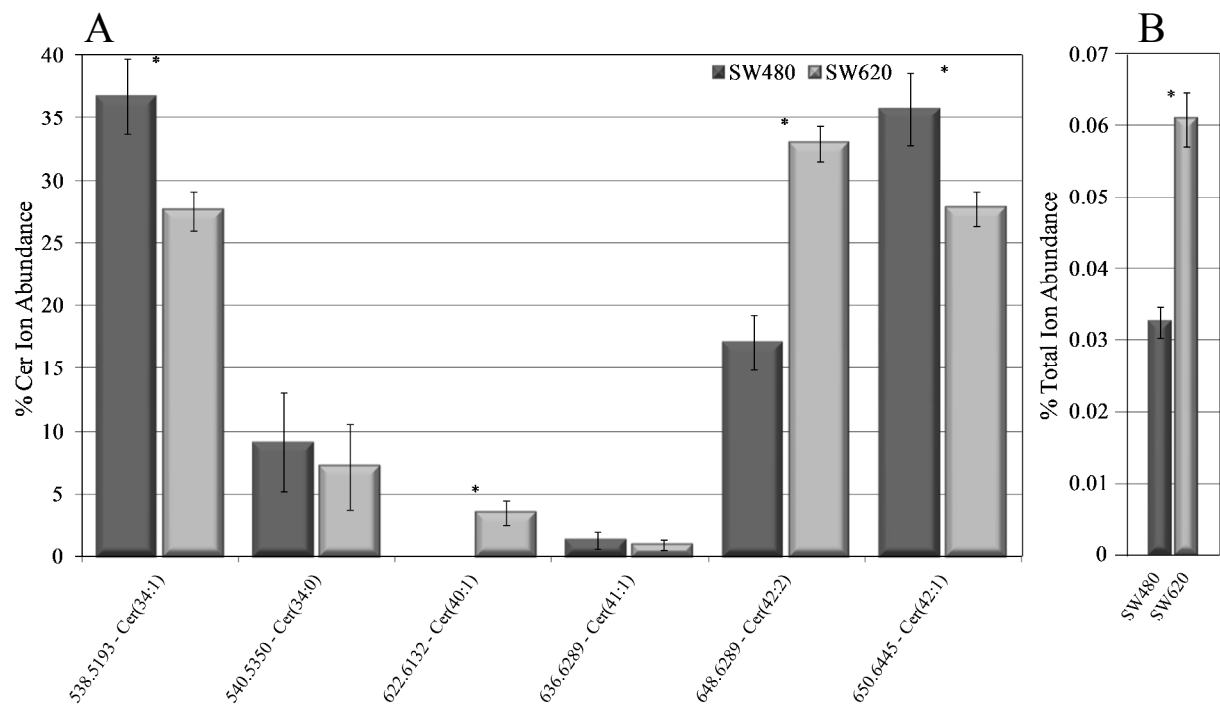
Figure S13. Quantification of Cer sphingolipids from the d_6-DMBNHS derivatized SW480 and SW620 cell crude lipid extracts. (A) Percent individual Cer ion abundances compared to the total ion abundance for all Cer lipids. (B) Percent total Cer ion abundance compared to the total ion abundance for all identified lipids. n = 5, * = p < 0.01.
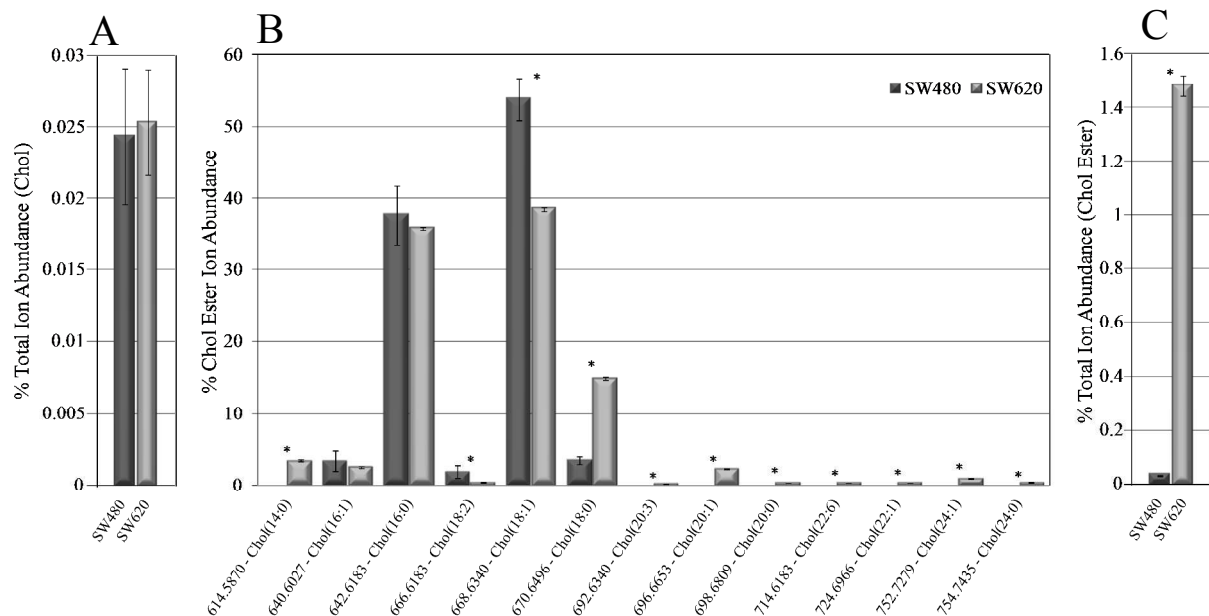
Figure S14. Quantification of cholesterol (Chol) and cholesterol esters (Chol ester) from the d_6-DMBNHS derivatized SW480 and SW620 cell crude lipid extracts. (A) Percent of total Chol ion abundance compared to the total ion abundance for all lipid peaks identified. (B) Percent individual Chol ester ion abundances compared to the total ion abundance for all Chol ester lipids. (C) Percent total Chol ester ion abundance compared to the total ion abundance for all identified lipids. n = 5, * = p < 0.01.
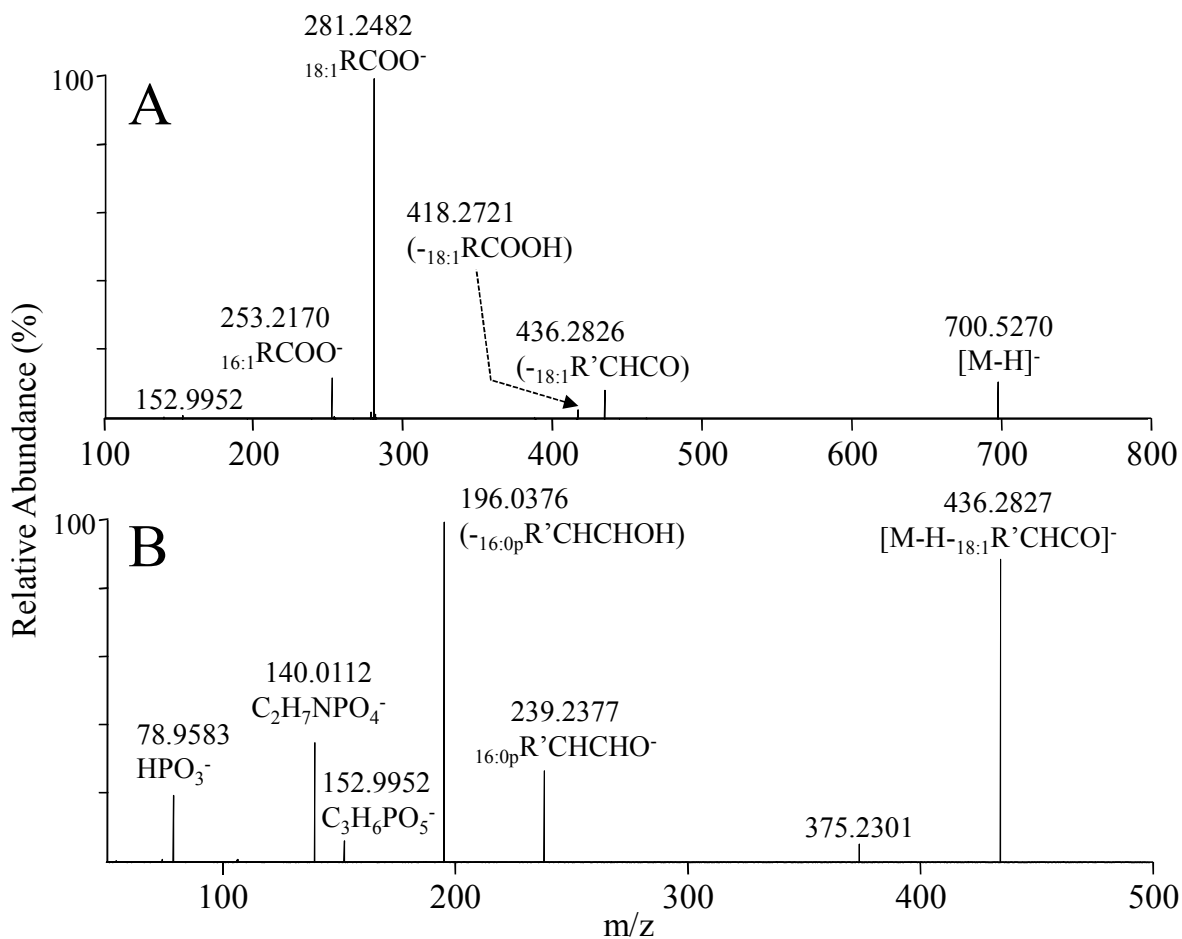
Figure S15. High resolution negative ionization mode HCD-MS/MS analysis of the underivatized deprotonated $PE_{(P-16:0/18:1)}$, $PE_{(O-16:1/18:1)}$, $PE_{(P-18:0/16:1)}$ and $PE_{(O-18:1/16:1)}$ lipids from the SW480 cell crude lipid extract. (A) ESI HCD-MS/MS of the $[M-H]^-$ precursor ion at m/z 700.5271, and (B) ESI CID-MS/MS followed by HCD-MS^3 of the m/z 436.3 ($-_{18:1}R'CHCO$) product ion from the $PE_{(P-16:0/18:1)}$ and $PE_{(O-16:1/18:1)}$ lipids from panel (A).